

Modelling and simulation of a bienzymatic reaction system co-immobilised within hydrogel-membrane liquid-core capsules

Ana Blandino*, Manuel Macías, Domingo Cantero

Biological and Enzymatic Reactors Research Group, Department of Chemical Engineering, Food Technology and Environmental Technologies, Faculty of Sciences, University of Cádiz (UCA), 11510 Puerto Real, Cádiz, Spain

Received 19 February 2002; accepted 14 May 2002

Abstract

A mathematical model applicable to the analysis and simulation of a heterogeneous bienzymatic reaction system is presented. The glucose oxidase–catalase (GOD–CAT) system co-encapsulated within hydrogel-membrane liquid-core capsules was chosen as the model system in this study. The proposed model considers a non-uniform biocatalyst concentration profile within the support and the deactivation phenomena of the two enzymes. Simulation experiments allowed us to elucidate the distribution of the two enzymes within the capsules. It seemed that GOD was distributed across the whole of the particle while CAT was confined almost exclusively to the core of the capsule. From the simulated glucose and hydrogen peroxide concentrations within the capsules, it was deduced that the hydrogen peroxide formed in the glucose oxidation reaction led firstly to the deactivation of the catalase and, after this point, GOD deactivation was accelerated. © 2002 Elsevier Science Inc. All rights reserved.

Keywords: Bienzymatic system; Co-encapsulation; Enzyme distribution; Deactivation; Mathematical model

1. Introduction

Immobilisation of enzymes onto insoluble supports has been one of the most exciting aspects of biotechnology. Immobilised enzymes offer a number of advantages over their soluble counterparts. Some of the more significant advantages of these systems include their reusability, especially if the enzymes are scarce or expensive, their applicability to continuous processes and the minimisation of pH and substrate-inhibition effects. In addition, retention of the enzyme in the bead avoids need for upstream enzyme makeup to the reactor and prevents downstream contamination of the product by residual enzyme. One way of immobilising enzymes is encapsulation within a gel matrix. In contrast to gel beads, capsules consist of a liquid core surrounded by a semipermeable membrane, which retains the biocatalyst within the capsule [1]. The main advantage of this immobilisation support lies in the specific particle structure, in which contact between the substrate and the biocatalyst can be achieved in an appropriate way, since the biocatalyst is in solution within the core of the capsule. As a consequence,

encapsulated enzymes have now found widespread application [2–4].

In recent years, a large number of authors have developed mathematical models, supported by experimental data, for bioreactors containing immobilised enzymes [5–9]. Simulation of these kinds of models leads to an improvement in the understanding and control of immobilised enzyme systems as well as the ability to predict the substrate consumption and product formation rates. However, such models are quite complex because they must consider the transport of substrates and products to and from the support, the enzymatic reaction in the immobilisation matrix, the biocatalyst deactivation phenomena and the enzyme distribution within the support.

The work described here concerns a theoretical model applicable to the analysis and simulation of a heterogeneous enzymatic process. The glucose oxidase–catalase (GOD–CAT) system co-encapsulated within hydrogel-membrane liquid-core capsules was chosen as the model system in this study. Both enzymes are related to natural processes because they participate in the enzymatic pool of those microorganisms able to oxidise glucose to gluconic acid. The action of GOD produces gluconic acid and hydrogen peroxide from glucose. The hydrogen peroxide, which causes the deactivation of both enzymes according

* Corresponding author. Tel.: +34-956-016381; fax: +34-956-016411.
E-mail address: ana.blandino@uca.es (A. Blandino).

Nomenclature	
$(K_M)_{CAT}$	Michaelis–Menten constant for H_2O_2 [$M L^{-3}$]
$(K_M)_{GOD}$	Michaelis–Menten constant for glucose [$M L^{-3}$]
D_P	Effective H_2O_2 diffusivity in the membrane of capsules [$L^2 T^{-1}$]
D_S	Effective glucose diffusivity in the membrane of capsules [$L^2 T^{-1}$]
E_C	Enzyme concentration within the core of capsules [$M L^{-3}$]
E_i	Enzyme concentration within a differential element of volume in the membrane of capsules [$M L^{-3}$]
E_t	Enzyme concentration in the reactor [$M L^{-3}$]
K	Parameter of enzyme distribution within the capsule (dimensionless)
K_{CAT}	Parameter of CAT distribution within the capsule (dimensionless)
K_{GOD}	Parameter of GOD distribution within the capsule (dimensionless)
$k_{i,CAT}$	Deactivation rate constant of CAT due to H_2O_2 [$M^{-1} L^3 T^{-1}$]
$k_{i,GOD}$	Deactivation rate constant of GOD due to H_2O_2 [$M^{-1} L^3 T^{-1}$]
$k_{0,CAT}$	Deactivation rate constant of CAT in the absence of H_2O_2 [T^{-1}]
$k_{0,GOD}$	Deactivation rate constant of GOD in the absence of H_2O_2 [T^{-1}]
k_p	Turnover number [T^{-1}]
N	Number of capsules
P	H_2O_2 concentration within the core capsule [$M L^{-3}$]
P_F	H_2O_2 feed concentration [$M L^{-3}$]
P_M	H_2O_2 concentration within a differential element of volume in the membrane of capsules [$M L^{-3}$]
P_R	H_2O_2 concentration in the bulk fluid [$M L^{-3}$]
Q	Volumetric flow rate [$L^3 T^{-1}$]
r	Radial co-ordinate in the capsule [L]
$r_{CAT}(c,t)$	H_2O_2 decomposition rate within the core of the capsule [$M L^{-3} T^{-1}$]
$r_{CAT}(r,t)$	H_2O_2 decomposition rate within a differential element of volume in the membrane of capsules [$M L^{-3} T^{-1}$]
R_e	External ratio of the gel membrane in the capsule [L]
$r_{GOD}(c,t)$	Glucose oxidation rate within the core of the capsule [$M L^{-3} T^{-1}$]
$r_{GOD}(r,t)$	Glucose oxidation rate within a differential element of volume in the membrane of capsules [$M L^{-3} T^{-1}$]
R_i	Internal ratio of the gel membrane in the capsule [L]
r_{max}	Maximum reaction rate for the free enzyme [$M L^{-3} T^{-1}$]
$r_{max}(c,0)$	Maximum reaction rate within the core of the capsule at $t = 0$ [$M L^{-3} T^{-1}$]
$r_{max}(r,0)$	Maximum reaction rate within a differential element of volume in the membrane of capsules at $t = 0$ [$M L^{-3} T^{-1}$]
$r_{max,CAT}$	Maximum H_2O_2 decomposition rate for free CAT [$M L^{-3} T^{-1}$]
$r_{max,CAT}(c,0)$	Maximum H_2O_2 decomposition rate within the core of the capsule at $t = 0$ [$M L^{-3} T^{-1}$]
$r_{max,CAT}(c,t)$	Maximum H_2O_2 decomposition rate within the core of the capsule [$M L^{-3} T^{-1}$]
$r_{max,CAT}(r,0)$	Maximum H_2O_2 decomposition rate within a differential element of volume in the membrane of the capsule at $t = 0$ [$M L^{-3} T^{-1}$]
$r_{max,CAT}(r,t)$	Maximum H_2O_2 decomposition rate within a differential element of volume in the membrane of capsules [$M L^{-3} T^{-1}$]
$r_{max,GOD}$	Maximum glucose oxidation rate for free GOD [$M L^{-3} T^{-1}$]
$r_{max,GOD}(c,0)$	Maximum glucose oxidation rate within the core of the capsule at $t = 0$ [$M L^{-3} T^{-1}$]
$r_{max,GOD}(c,t)$	Maximum glucose oxidation rate within the core of the capsule [$M L^{-3} T^{-1}$]
$r_{max,GOD}(r,0)$	Maximum glucose oxidation rate within a differential element of volume in the membrane of the capsule at $t = 0$ [$M L^{-3} T^{-1}$]
$r_{max,GOD}(r,t)$	Maximum glucose oxidation rate within a differential element of volume in the membrane of capsules [$M L^{-3} T^{-1}$]
S	Glucose concentration within the core capsule [$M L^{-3}$]
S_F	Glucose feed concentration [$M L^{-3}$]
S_M	Glucose concentration within a differential element of volume in the membrane of capsules [$M L^{-3}$]
S_R	Glucose concentration in the bulk fluid [$M L^{-3}$]
t	Time [T]
V_L	Bulk fluid volume [L^3]

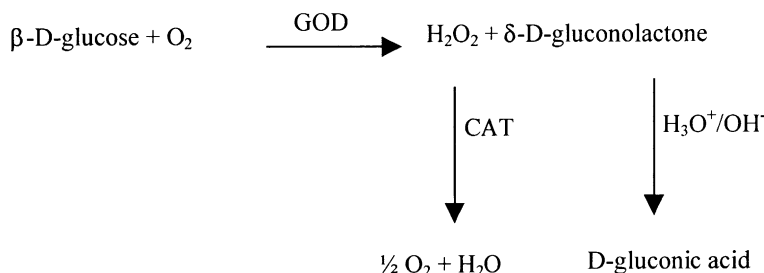


Fig. 1. Reaction mechanism of the glucose oxidase–catalase system.

to first-order kinetics [10,11], is then split into oxygen and water with the aid of CAT (Fig. 1).

Unlike traditional models applied to enzymatic processes, the proposed model considers a non-uniform biocatalyst concentration profile within the support and the deactivation phenomena of the two enzymes. Theoretical investigations have shown that enzyme distribution within the support can have a significant effect on the observed reaction rates. In this way, Celayeta et al. have reported that in the case of sequential reactions catalysed by co-immobilised enzymes, the two enzymes distribution within the support plays an important role in the maximum yield of the final product [12]. Nevertheless, in most cases the mathematical model assumes that the enzyme is uniformly distributed throughout the support structure. The consideration of the non-uniform biocatalyst concentration profile within the support is quite a recent development and only a few papers have described theoretical models that incorporate this factor [13–15]. The validity of the model proposed here has been tested by comparing the predicted results with experimental data for substrate (glucose) and product (hydrogen peroxide) concentrations in the reactor. The final product, gluconic acid, is not important in terms of the present analysis.

2. Mathematical model

The proposed model is based on the idea that the substrates diffuse from the liquid phase to the solid support, where they are consumed to yield the products that will diffuse from the solid matrix to the liquid medium. The nature of the capsules allows the substrates and the products to diffuse in and out, respectively, but the enzymes are retained inside. A schematic representation of a spherical capsule is shown in Fig. 2.

2.1. Enzyme distribution within the capsules

In the development of the theoretical model, it has been assumed that enzymes are distributed between the core and the membrane of the capsules. This hypothesis has been arrived at by considering previous experimental studies into the diffusion of GOD and CAT from calcium alginate gel

capsules. It was found that a small percentage of GOD leaked from the capsules while CAT release was not detected (data not shown). GOD leakage from the capsules was explained as being the result of the incorporation of the enzyme within the capsule membrane during its formation. When gelation occurs during capsule formation, water is expelled from the capsules because the gel contracts during crosslinking. Water migrates to the bead surface and this flux may carry enzyme molecules that become trapped within the gel membrane of the capsules [16]. It was, therefore, believed that a certain percentage of the enzymes could be retained within the membrane of the capsule.

A homogeneous and an exponential enzyme distribution were defined at the liquid core and at the membrane of the capsule, respectively. The selection of this kind of enzyme concentration profile at the membrane was based on the literature data, which reveal an exponential form for the distribution of immobilised enzymes in some porous supports [14,15]. Taking into account these findings, the following empirical equation was proposed to describe the distributions of the two enzymes within the capsules:

$$E_i = E_C \left[1 - \exp \left[-K \left(\frac{R_e - r}{r - R_i} \right) \right] \right] \quad (1)$$

where E_i is defined as the active enzyme concentration within a differential element of volume in the membrane and E_C represents the active enzyme concentration within

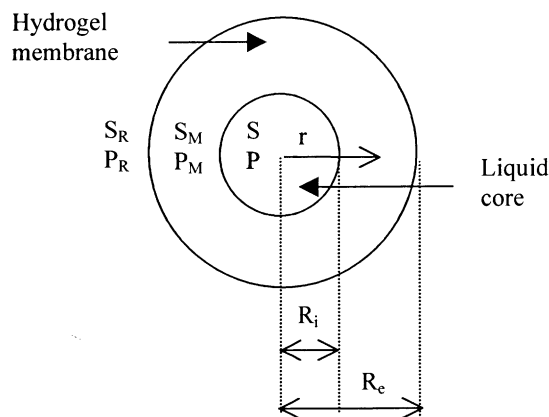


Fig. 2. Schematic view of a capsule particle.

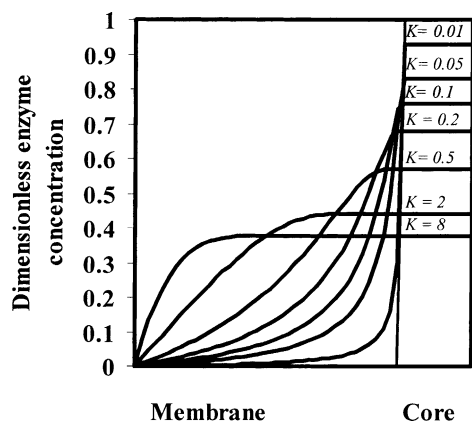


Fig. 3. Dimensionless enzyme concentration profile in the capsule as a function of the parameter K .

the capsule core. R_e and R_i are the external and the internal ratio of the gel membrane, respectively, and r is the radial co-ordinate in the capsules. K is a non-dimensional parameter that allows the modification of the enzyme distribution in the capsules.

The molecular weights of GOD and CAT are quite different (GOD = 152,000 Da; CAT = 232,000 Da) and so different distributions of the two enzymes within the capsules would be expected. Consequently, two different parameters were defined for GOD and CAT distributions (K_{GOD} and K_{CAT}). Fig. 3 shows the evolution of the dimensionless enzyme concentration in a capsule for different K values. The enzyme concentrations at different positions in the capsule were made non-dimensional by dividing each value by the resulting enzyme concentration, if all the enzyme molecules in the capsule were confined in the core. It can be seen from this figure that, as K increases, the amount of enzyme contained within the membrane of the capsule also increases.

2.2. Formulation of the mathematical model

The following assumptions were made in developing the model:

- The reactor is assumed to be perfectly mixed and isothermal conditions are maintained.
- The capsules are suspended in the reactor in a uniform manner.
- The enzymes are included exclusively within the capsules, presenting a homogeneous distribution within the core and an exponential distribution within the membrane.
- The mass-transfer resistance between the solution and external surface of the capsule is negligible.
- The diffusion of substrates and products inside the membrane of the capsules can be modelled by Fick's first law, and effective diffusivities are constant.
- Substrate and product concentration profiles are negligible within the core of the capsule.

- External and internal oxygen transfer rates within the reactor are sufficiently high that they are not determining factors in the global reaction rate.

2.3. Mathematical model equations

2.3.1. Mass balances within the capsules

A differential unsteady state mass balance for the substrate and the product based on the above assumptions in the core of the capsules gives:

$$-\frac{3D_S}{R_i} \frac{\partial S_M}{\partial r} \Big|_{r=R_i} = r_{\text{GOD}}(c, t) + \frac{dS}{dt}, \quad (2)$$

$$\frac{3D_P}{R_i} \frac{\partial P_M}{\partial r} \Big|_{r=R_i} = r_{\text{CAT}}(c, t) - r_{\text{GOD}}(c, t) + \frac{dP}{dt} \quad (3)$$

and in the membrane of the capsules gives:

$$D_S \left(\frac{\partial^2 S_M}{\partial r^2} + \frac{2}{r} \frac{\partial S_M}{\partial r} \right) = \frac{\partial S_M}{\partial t} + r_{\text{GOD}}(r, t), \quad (4)$$

$$D_P \left(\frac{\partial^2 P_M}{\partial r^2} + \frac{2}{r} \frac{\partial P_M}{\partial r} \right) = \frac{\partial P_M}{\partial t} + r_{\text{CAT}}(r, t) - r_{\text{GOD}}(r, t). \quad (5)$$

2.3.2. Mass balances in the bulk fluid phase

An unsteady state mass balance of the substrate and the product in the bulk fluid phase of the continuous stirred tank reactor gives:

$$Q_{S_F} - Q_{S_R} = -ND_S 4\pi R_e^2 \frac{\partial S_M}{\partial r} \Big|_{r=R_e} + V_L \frac{dS_R}{dt}, \quad (6)$$

$$Q_{P_F} - Q_{P_R} = ND_P 4\pi R_e^2 \frac{\partial P_M}{\partial r} \Big|_{r=R_e} + V_L \frac{dP_R}{dt}. \quad (7)$$

For the experiments in the batch stirred tank reactor, Eqs. (6) and (7) can be simplified as follows:

$$ND_S 4\pi R_e^2 \frac{\partial S_M}{\partial r} \Big|_{r=R_e} = V_L \frac{dS_R}{dt}, \quad (8)$$

$$-ND_P 4\pi R_e^2 \frac{\partial P_M}{\partial r} \Big|_{r=R_e} = V_L \frac{dP_R}{dt}. \quad (9)$$

2.3.3. Reaction rate expressions

In previous studies, it was experimentally determined that the rate of D-glucose oxidation by encapsulated GOD, under air-saturated oxygen conditions, could be expressed according to the Michaelis–Menten kinetic law [17]. In the proposed model, two similar equations have been defined for glucose oxidation within the core and within a differential element of volume in the membrane of the capsule:

$$r_{\text{GOD}}(c, t) = \frac{r_{\text{max GOD}}(c, t)S}{(K_M)_{\text{GOD}} + S}, \quad (10)$$

$$r_{\text{GOD}}(r, t) = \frac{r_{\text{max GOD}}(r, t)S_M}{(K_M)_{\text{GOD}} + S_M}. \quad (11)$$

$$r_{\max \text{ CAT}}(r, 0) = \frac{V_L}{N(4/3)\pi R_i^3 \left[1 + (3/R_i^3) \int_{r=R_i}^{r=R_e} r^2 [1 - \exp[-K(R_e - r)/(r - R_i)]] dr \right]} r_{\max \text{ CAT}}, \quad (20)$$

Similarly, the following equations were established for the decomposition of hydrogen peroxide by CAT:

$$r_{\text{CAT}}(c, t) = \frac{r_{\max \text{ CAT}}(c, t) P}{(K_M)_{\text{CAT}} + P}, \quad (12)$$

$$r_{\text{CAT}}(r, t) = \frac{r_{\max \text{ CAT}}(r, t) P_M}{(K_M)_{\text{CAT}} + P_M}. \quad (13)$$

In the above equations, both GOD and CAT deactivation kinetics and the distributions of the two enzymes within the capsules were included in the formulation of the parameters $r_{\max \text{ GOD}}(r, t)$, $r_{\max \text{ GOD}}(c, t)$, $r_{\max \text{ CAT}}(r, t)$ and $r_{\max \text{ CAT}}(c, t)$ as described below.

2.3.3.1. Integration of the enzyme distribution in the rate expressions. If it is assumed that the enzyme is exclusively distributed between the core and the membrane of the capsule, the following expression can be obtained:

$$V_L E_t = N \frac{4}{3} \pi R_i^3 E_c + N \int_{r=R_i}^{r=R_e} 4\pi r^2 E_c \times \left[1 - \exp \left[-K \left(\frac{R_e - r}{r - R_i} \right) \right] \right] dr. \quad (14)$$

Eq. (14) can be rewritten as follows:

$$E_c = \frac{V_L E_t}{N(4/3)\pi R_i^3 \left[1 + (3/R_i^3) \int_{r=R_i}^{r=R_e} r^2 [1 - \exp[-K(R_e - r)/(r - R_i)]] dr \right]}. \quad (15)$$

If the terms in Eq. (15) are multiplied by the turnover number, k_p , it is possible to obtain the value of the maximum reaction rate within the core of capsules as a function of the value of this parameter for the free enzyme:

$$r_{\max}(c, 0) = \frac{V_L}{N(4/3)\pi R_i^3 \left[1 + (3/R_i^3) \int_{r=R_i}^{r=R_e} r^2 [1 - \exp[-K(R_e - r)/(r - R_i)]] dr \right]} r_{\max}. \quad (16)$$

The above equation is defined for $t = 0$, at which point deactivation phenomena of the enzymes are not evident. In the same way, for a differential element of volume within the membrane of the capsules, the following expression can be obtained:

$$r_{\max}(r, 0) = \left[1 - \exp \left[-K \left(\frac{R_e - r}{r - R_i} \right) \right] \right] r_{\max}(c, 0). \quad (17)$$

Therefore, for the enzymes GOD and CAT the following equations can be obtained:

$$r_{\max \text{ GOD}}(c, 0) = \frac{V_L}{N(4/3)\pi R_i^3 \left[1 + (3/R_i^3) \int_{r=R_i}^{r=R_e} r^2 [1 - \exp[-K(R_e - r)/(r - R_i)]] dr \right]} r_{\max \text{ GOD}}, \quad (18)$$

$$r_{\max \text{ GOD}}(r, 0) = \left[1 - \exp \left[-K \left(\frac{R_e - r}{r - R_i} \right) \right] \right] r_{\max \text{ GOD}}(c, 0), \quad (19)$$

$$r_{\max \text{ CAT}}(r, 0) = \left[1 - \exp \left[-K \left(\frac{R_e - r}{r - R_i} \right) \right] \right] r_{\max \text{ CAT}}(c, 0). \quad (21)$$

2.3.3.2. Integration of the enzyme deactivation kinetics in the reaction rate expressions. A survey of the literature shows that first-order rate equations can be assumed to describe the irreversible deactivation by hydrogen peroxide of co-immobilised GOD and CAT. In this respect, Tse and Gough's model provides the following equation [10]:

$$\frac{dE_t}{dt} = -(k_0 + k_i P_R) E_t \quad (22)$$

where E_t is the concentration of active enzyme, P_R is the concentration of hydrogen peroxide, k_0 is the deactivation rate constant in the absence of hydrogen peroxide, and k_i is the rate constant of deactivation due to hydrogen peroxide.

On the other hand, given that the parameter r_{\max} is directly related to the enzyme concentration, Eq. (22) can be rewritten for GOD and CAT as follows:

$$\frac{dr_{\max \text{ GOD}}(c, t)}{dt} = -(k_0 \text{ GOD} + k_i \text{ GOD} P) r_{\max \text{ GOD}}(c, t), \quad (23)$$

$$\frac{dr_{\max \text{ GOD}}(r, t)}{dt} = -(k_0 \text{ GOD} + k_i \text{ GOD} P_M) r_{\max \text{ GOD}}(r, t), \quad (24)$$

$$\frac{dr_{\max \text{ CAT}}(c, t)}{dt} = -(k_0 \text{ CAT} + k_i \text{ CAT} P) r_{\max \text{ CAT}}(c, t), \quad (25)$$

$$\frac{dr_{\max \text{ CAT}}(r, t)}{dt} = -(k_0 \text{ CAT} + k_i \text{ CAT} P_M) r_{\max \text{ CAT}}(r, t) \quad (26)$$

where $k_0 \text{ GOD}$ and $k_0 \text{ CAT}$ are the deactivation rate constants in the absence of hydrogen peroxide for GOD and CAT, respectively, and $k_i \text{ GOD}$ and $k_i \text{ CAT}$ are the rate constants of deactivation due to hydrogen peroxide for the two enzymes.

2.3.4. Initial and boundary conditions

The initial conditions are:

$$t = 0, \quad 0 \leq r < R_e, \quad S_M = S = 0, \quad P_M = P = 0; \quad (27)$$

$$t = 0, \quad r = R_e, \quad S_M = S_F, \quad P_M = P_F; \quad (28)$$

$$t = 0, \quad S_R = S_F, \quad P_R = P_F. \quad (29)$$

In addition, Eqs. (18)–(21) are included in the group of initial conditions of the system.

The boundary conditions in the capsules are defined as follows:

$$\text{at a given time } t, \quad r = R_e, \quad S_M = S_R, \quad P_M = P_R; \quad (30)$$

$$\text{at a given time } t, \quad r = R_i, \quad S_M = S, \quad P_M = P. \quad (31)$$

3. Experimental

3.1. Materials

Sodium alginate and the sodium salt of carboxymethyl-cellulose (CMC) were provided by Fluka BioChemika, Switzerland (Fluka 71238 and Fluka 21902, respectively). Anhydrous calcium chloride (purissimum grade) was used as the calcium salt for capsule formation (Panreac 141219).

Glucose oxidase (EC 1.1.3.4) and catalase (EC 1.11.1.6) were purchased from the Sigma Chemical Co., USA (SIGMA G 7141 and SIGMA C 3515, respectively). The substrate D-(+)-glucose was supplied by Panreac, Spain (Panreac 141341). All other chemicals were commercially available products of reagent grade.

3.2. Enzyme encapsulation procedure

Calcium alginate capsules (7.80 ± 0.05 mm in diameter and with a membrane thickness of 1.15 ± 0.02 mm) were prepared by extrusion using the previously described method [17]. Alginate solution (1%, w/v) was used as the anionic solution and CMC (3%, w/v) dissolved in CaCl_2 (5.5%, w/v) was employed as the cationic solution. The enzymes were dissolved in the cationic solution. Droplets of the cationic solution were dropped, through a silicone tube (1.6 mm in diameter) using a peristaltic pump, into 200 ml of sodium alginate solution under constant stirring (330 rpm). The dropping height was 10 cm and the gelation time, or period in which capsules were formed, was 1 h.

3.3. Kinetics studies and experimental apparatus

The kinetics of both glucose oxidation and hydrogen peroxide decomposition by free GOD and free CAT were studied in batch operation mode. Kinetics were studied by measuring the change in the concentration of glucose and hydrogen peroxide by means of a spectrometric assay. The glucose and hydrogen peroxide concentrations were varied from 10 to 125 mM in the buffer solution. All solutions were freshly prepared in 50 mM calcium acetate buffer (pH 5.1) made up with distilled demineralised water. These experiments allowed us to calculate the maximum

reaction rates and the Michaelis constants for the two enzymes.

The performance of the co-immobilised GOD–CAT system was studied in both batch and continuous operation mode.

The equipment for batch experiments consisted of an automatic, thermostatically controlled reactor (APPLIKON ADI 1030) equipped with an aeration system, mechanical agitation and a sample collector. Automatic control was achieved using a PID computer system. The reactor was constructed of glass and had a capacity of 5.2 l and a working volume of 3 l. The equipment was operated with an aeration rate of 1 vvm and a stirring rate of 300 rpm. The temperature was kept constant at 35 °C using a cooling/heating bath with an accuracy of ± 0.1 °C.

The equipment for continuous experiments consisted of a glass reactor (300 ml total volume with a working volume of 250 ml) in conjunction with mechanical stirring and a water jacket. The temperature of operation and the aeration and agitation rates were fixed at the same values as in the equipment used for batch experiments.

In all the experiments, the same protocol for bioreactor start up was carried out. The solution of glucose in calcium acetate buffer was introduced into the bioreactor and the capsules were added. This instant was considered as $t = 0$ in all experiments. At $t = 0$ and subsequent different time intervals, 1 ml of sample was automatically taken from the reactor by a fraction collector and glucose and hydrogen peroxide concentrations were measured. All experiments were carried out under air-saturated oxygen conditions.

3.4. Analytical methods

Glucose was determined by the dinitrosalicylic acid method [18]. The hydrogen peroxide concentration was measured using the method described by Boltz and Howell [19]. The oxygen concentration was measured with a Clark electrode.

4. Results and discussion

4.1. Model integration

The model set of Eqs. (2)–(13) and (23)–(26) were solved by numerical procedures using finite differences and fourth-order Runge–Kutta methods. The computer program used to perform the calculations was written in Visual Basic and the input consisted of the values of the process variables and parameters given in Table 1. The numeric output of the program is the concentration of the substrate (glucose) and product (hydrogen peroxide) in the bulk fluid phase of the reactor and within the core and the membrane of the capsules as a function of time.

Apparent diffusivity values of glucose (D_S) and hydrogen peroxide (D_P) were established according to literature

Table 1
Model parameters and experimental conditions

Parameter	Value
Reactor	
Q	$2.78 \times 10^{-8} \text{ m}^3/\text{s}$
S_F	$14 \text{ mol}/\text{m}^3$
P_F	$0 \text{ mol}/\text{m}^3$
Capsules	
R_e	$3.9 \times 10^{-3} \text{ M}$
R_i	$2.75 \times 10^{-3} \text{ M}$
D_S	$6.8 \times 10^{-10} \text{ m}^2/\text{s}$
D_P	$1.0 \times 10^{-9} \text{ m}^2/\text{s}$
K_{GOD}	8
K_{CAT}	0.1
Reaction	
$r_{\text{max GOD}}$	$0.96 \text{ mol}/\text{m}^3 \text{ s}$
$r_{\text{max CAT}}$	$2.09 \text{ mol}/\text{m}^3 \text{ s}$
$(K_M)_{\text{GOD}}$	$18 \text{ mol}/\text{m}^3$
$(K_M)_{\text{CAT}}$	$238 \text{ mol}/\text{m}^3$
$k_0 \text{ GOD}$	$1.7 \times 10^{-8} \text{ s}^{-1}$
$k_i \text{ GOD}$	$8.3 \times 10^{-6} \text{ m}^3/\text{mol s}$
$k_0 \text{ CAT}$	$1.7 \times 10^{-6} \text{ s}^{-1}$
$k_i \text{ CAT}$	$3.3 \times 10^{-4} \text{ m}^3/\text{mol s}$

data [20,21]. Michaelis–Menten kinetic studies from initial rate experiments for both free GOD and CAT allowed us to calculate the parameters $r_{\text{max GOD}}$, $r_{\text{max CAT}}$, $(K_M)_{\text{GOD}}$ and $(K_M)_{\text{CAT}}$. The numerical solutions provided by the model

were fitted by non-linear regression to the experimental data (glucose and hydrogen peroxide concentrations versus time) and allowed the estimation of the values of the parameters K_{GOD} and K_{CAT} and the deactivation rate constants for the two enzymes.

4.2. Simulation results

Fig. 4 shows the degree of correlation between the experimentally measured and theoretically calculated substrate and product concentrations in the liquid phase of the bioreactors under different experimental conditions. Model parameters and experimental conditions employed for the simulation experiments are included in Table 1. As can be seen from the figures mentioned above, the experimental trends followed by glucose and hydrogen peroxide concentrations in the reactors were found to be in agreement with the theoretical predictions, although some discrepancies between simulated and experimental data could be observed. Nevertheless, considering the large number of ideal suppositions that were assumed in the development of the theoretical model, such differences are not unexpected.

The simulations allowed us to gain a more in-depth view of the kinetic behaviour of the enzymatic system GOD–CAT. Simulation experiments allowed us to ascertain the concentration distributions of the two enzymes within the capsules. In this respect, the presence of the enzymes in both the

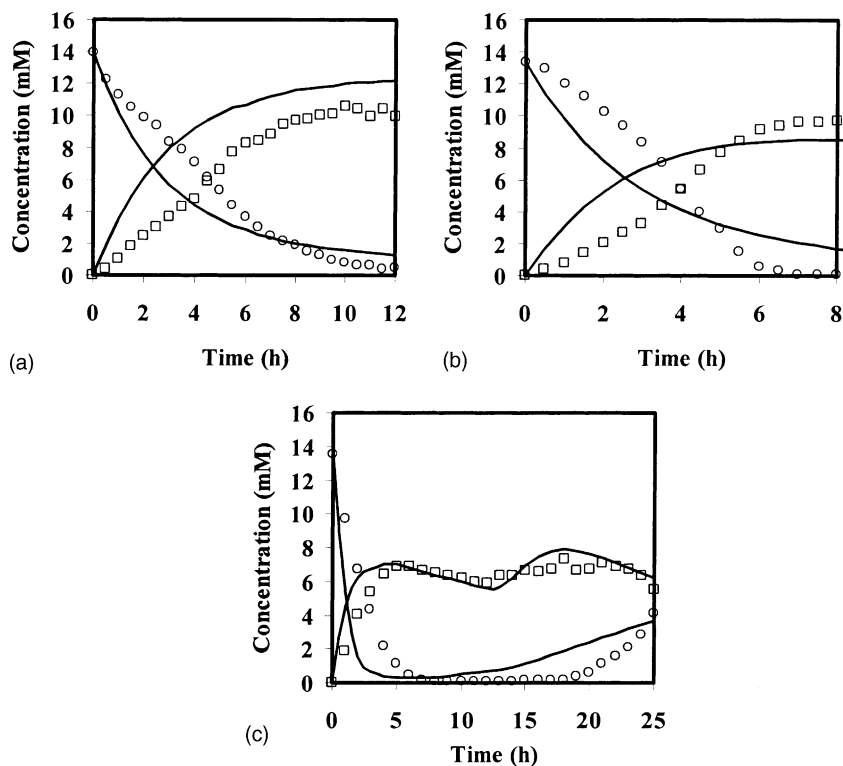


Fig. 4. Kinetics of D-glucose oxidation (○) and hydrogen peroxide formation (□) by encapsulated GOD in the batch stirred tank reactor (a), co-encapsulated GOD–CAT system in the batch stirred tank reactor (b) and co-encapsulated GOD–CAT system in the continuous stirred tank reactor (c). Experimental data (points) and simulated data (solid lines).

membrane and the core of the capsules was one of the hypotheses that was assumed during the formulation of the model. This hypothesis could be ratified by considering the different values assigned for the parameters K_{GOD} and K_{CAT} , which indicate that the two enzyme distributions were quite different. It seemed that GOD was distributed throughout the whole particle ($K_{\text{GOD}} = 8$) while CAT was confined almost exclusively to the core of the capsule ($K_{\text{CAT}} = 0.1$) (Fig. 3). If we consider the molecular weights of GOD and CAT, these differences in the concentration profiles of the two enzymes are not unexpected.

In the same way, the simulation experiments provide information about the substrate and the product profiles within the capsules. As an example, Fig. 5 shows the results of a simulated experiment with the co-encapsulated GOD–CAT system in the continuous stirred tank reactor. (Fig. 5a and c) illustrates the simulated temporal evolution of glucose and hydrogen peroxide concentrations in both the liquid phase of the reactor and within the liquid core of the capsules. (Fig. 5b and d) shows the glucose and hydrogen peroxide concentration profiles within the membrane of the capsules.

As far as the glucose concentration in the reactor is concerned (Fig. 5a), four stages can be clearly observed. Ini-

tially, the glucose concentration decreases in a linear fashion with time before decreasing less sharply and reaching values very close to zero. About 8 h after the initiation of the process, a linear increase in glucose concentration is observed. This increase becomes more marked during the fourth stage, which begins at the point 15 h after the process had commenced. During the first two stages, the glucose concentration is zero (or almost zero) in both the membrane (Fig. 5b) and the liquid core of the capsules (Fig. 5c). This situation indicates that most of the GOD enzymes must be in an active state and, consequently, all the glucose molecules that diffuse into the capsules are oxidised. On the other hand, considering that a reasonably large percentage of GOD is trapped within the membrane, most of the glucose molecules that diffuse from the liquid phase of the reactor to the capsules are probably oxidised at the membrane. However, 15 h after the process has started, glucose begins to accumulate within the capsules, demonstrating that most of the GOD enzyme molecules are probably in an inactive state.

With regard to the hydrogen peroxide concentration in the reactor, four stages are again observed (Fig. 5a). In the first stage, the concentration of hydrogen peroxide increases rapidly and reaches a maximum value after about 5 h.

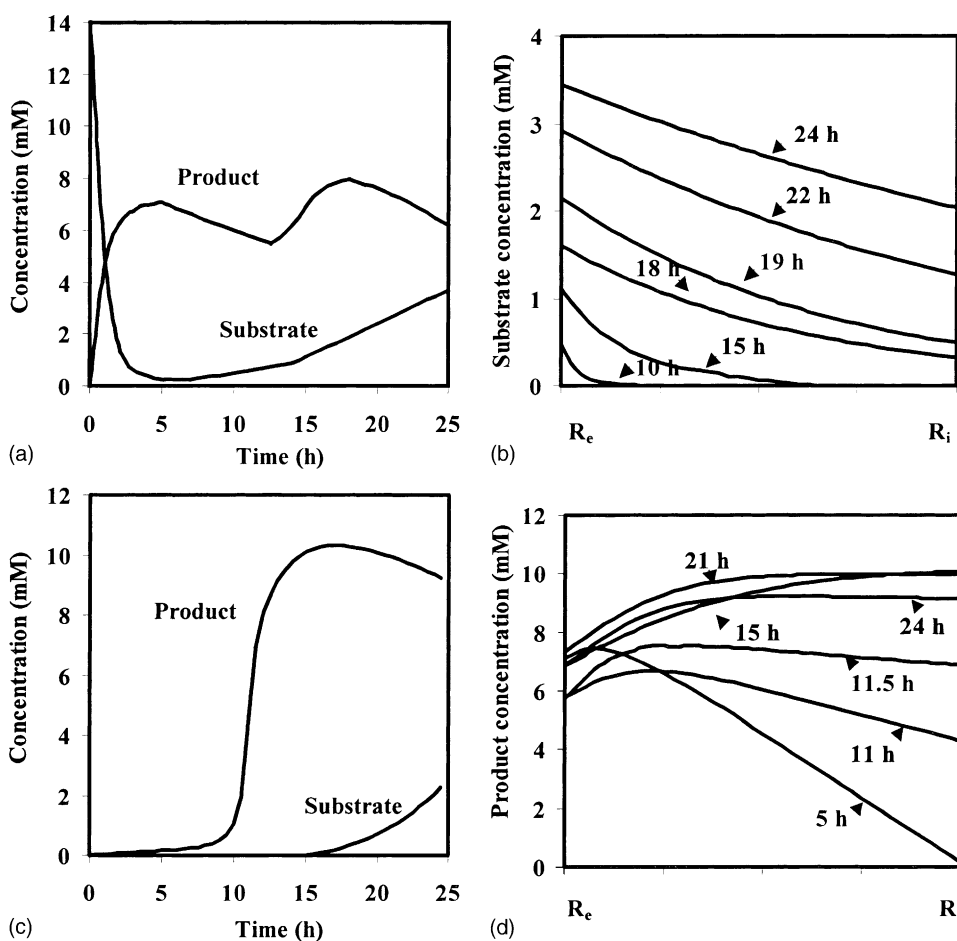


Fig. 5. Temporal evolution of the simulated substrate (D-glucose) and product (hydrogen peroxide) concentrations in the liquid phase of the continuous stirred tank reactor (a); within the liquid core of the capsules (c); and within the membrane of the capsules (b) and (d).

During this period of time, a sharp increase in the hydrogen peroxide concentration within the membrane is also observed (Fig. 5d). However, the hydrogen peroxide concentration within the core is virtually zero (Fig. 5c); a result that is expected considering that most of the CAT enzyme is confined within the core. The hydrogen peroxide that is not decomposed within the capsules diffuses into the solution. In the second stage, a decrease in hydrogen peroxide concentration is observed in the liquid phase of the reactor (Fig. 5a), indicating that CAT decomposes the hydrogen peroxide formed in the capsules and also some proportion of the hydrogen peroxide accumulated in the reactor. Between 10 and 12 h after the process has started, a very sharp increase in the hydrogen peroxide concentration at the core is observed (Fig. 5c), indicating that CAT deactivation phenomena caused by its own substrate are evident. As a consequence, hydrogen peroxide begins to accumulate within the capsules.

At the third stage, about 12 h after the process has started, the hydrogen peroxide concentration increases continuously in the reactor (Fig. 5a), meaning that most of the CAT molecules have probably been deactivated. Nevertheless, at this stage the glucose concentration in the reactor is sufficiently low to suppose that a high percentage of GOD is in an active state. Once most of the CAT molecules have been deactivated, as the hydrogen peroxide accumulation on the capsules is quite significant, GOD deactivation phenomena are accelerated and glucose is accumulated in the reactor. These results, therefore, indicate that the hydrogen peroxide formed in the glucose oxidation reaction deactivates CAT first. After this process has occurred, GOD deactivation is accelerated.

Finally, in the fourth stage, a decrease in the hydrogen peroxide concentration is observed in the reactor, a situation that is thought to be due to washout phenomena.

5. Conclusions

The work described here concerns a theoretical model applicable to the analysis and simulation of stirred tank reactors operating with co-encapsulated enzyme systems. The model considers the transport of substrates and products to and from the capsules, the enzymatic reactions in the immobilisation matrix, the biocatalysts deactivation phenomena and the enzymes distributions within the capsules. An empirical exponential equation was proposed to describe the distribution of the two enzymes within the capsules. The variation of the parameter K included in the above equation allowed the modification of the enzymes distribution in the capsules. The deactivation kinetics and the distributions of the two enzymes within the capsules were included in the formulation of the reaction rate expressions. The model set of equation were solved by numerical procedures using finite differences and fourth-order Runge–Kutta methods. Diffusivities of the substrate and the product were estab-

lished according to literature data, the kinetic parameters of reaction rate expressions were obtained by experiments, while the parameter K for the two enzymes and the deactivation rate constants were estimated by fitting the numerical solutions to experimental data by non-linear regression analysis. Therefore, series of different experiments were carried out using GOD and CAT co-immobilised within calcium alginate gel capsules. The simulations experiments allowed us to ratified the main hypotheses that was assumed during the formulation of the model: the non-uniform biocatalyst concentration profile within the support.

References

- [1] Nigam SC, Tsao IF, Sakoda A, Wang HY. Techniques for preparing hydrogel membrane capsules. *Biotechnol Tech* 1988;2: 271–6.
- [2] Levee MG, Lee GM, Paek SH, Paison BO. Microencapsulated narrow cultures: a potential culture system for the clonal outgrowth of hematopoietic progenitor cells. *Biotechnol Bioeng* 1994;43: 734–9.
- [3] Jankowski T, Zielinska M, Wysakowska A. Encapsulation of lactic acid bacteria with alginate/starch capsules. *Biotechnol Tech* 1997;11:31–4.
- [4] Tay LF, Khoh LK, Loh CS, Khor E. Alginate-Chitosan coacervation in production of artificial seeds. *Biotechnol Bioeng* 1993;42: 449–54.
- [5] Ladero M, Santos A, García-Ochoa F. Kinetic modelling of lactose hydrolysis with an immobilized-galactosidase from *Kluyveromyces fragilis*. *Enzyme Microb Technol* 2000;27:583–92.
- [6] García R, García T, Martínez M, Aracil J. Kinetic modelling of the synthesis of 2-hydroxy-5-hexenyl 2-chlorobutyrate ester by an immobilised lipase. *Biochem Eng J* 2000;5:185–90.
- [7] Pal P, Datta S, Bhattacharya P. Studies on the modelling and simulation of a sequential bienzymatic reaction system immobilized in emulsion liquid membrane. *Biochem Eng J* 2000;5:89–100.
- [8] Pibyl M, Chmelíková R, Hasal P, Marek M. Modeling of hydrogel immobilized enzyme reactors with mass-transport enhancement by electric field. *Chem Eng Sci* 2001;56:433–42.
- [9] Pal P, Datta S, Bhattacharya P. Studies on the modeling and simulation of a sequential bienzymatic reaction system immobilized in emulsion liquid membrane. *Biochem Eng J* 2000;5:89–100.
- [10] Tse PHS, Gough DA. Time-dependent inactivation of immobilized glucose oxidase and catalase. *Biotechnol Bioeng* 1987;29: 705–13.
- [11] Malikkides CO, Weiland RH. On the mechanism of immobilized glucose oxidase deactivation by hydrogen peroxide. *Biotech Bioeng* 1982;24:2419–39.
- [12] Celayeta JF, Silva AH, Balcao VM, Malcata FX. Maximisation of the yield of final product on substrate in the case of sequential reaction catalysed by coimmobilised enzymes: a theoretical analysis. *Bioprocess Biosyst Eng* 2001;24:143–9.
- [13] Hassan MM, Beg SA, Chowdhury MHM, Atiqullah M. Analysis of non-isothermal tubular reactor packed with immobilized enzyme systems. *Biochem Eng J* 1995;58:275–83.
- [14] Dalvie SK, Baltus RE. Distribution of immobilized enzymes on porous membranes. *Biotechnol Bioeng* 1992;40:1173–80.
- [15] Hossain MdM, Do DD. Determination of intraparticle immobilized enzyme distribution under moderate diffusion conditions. *Biotechnol Bioeng* 1992;40:747–9.

- [16] Blandino A, Macías M, Cantero D. Glucose oxidase release from calcium alginate gel capsules. *Enzyme Microb Technol* 2000;27: 319–24.
- [17] Blandino A, Macías M, Cantero D. Immobilization of glucose oxidase within calcium alginate gel capsules. *Process Biochem* 2001;36: 601–6.
- [18] Miller GL. Use of dinitrosalicylic acid reagent for determination of reducing sugar. *Anal Chem* 1959;31:426–8.
- [19] Boltz DF, Howell JA. In: Boltz DF, Howell JA, editors. *Colorimetric determination of non metals*. New York: Wiley, 1987. p. 543.
- [20] Venancio A, Teixeira V. Characterization of sugar diffusion coefficients in alginate membranes. *Biotechnol Tech* 1997;11: 183–5.
- [21] Mikkelsen SR, Lennox RB. Rotating disc electrode characterization of immobilized glucose oxidase. *Ann Biochem* 1991;195:358–63.